

A Single-Site Mutation (F429H) Converts the Enzyme CYP 2B4 into a Heme Oxygenase: A QM/MM Study

Dandamudi Usharani,[†] Costantino Zazza,[‡] Wenzhen Lai,^{†,||} Mukesh Chourasia,[†] Lucy Waskell,^{*,§} and Sason Shaik^{*,†}

[†]Institute of Chemistry and the Lise Meitner-Minerva Center for Computational Quantum Chemistry, The Hebrew University of Jerusalem, 91904 Jerusalem, Israel

[‡]Scuola Normale Superiore di Pisa, Piazza dei Cavalieri 7, 56126 Pisa, Italy

[§]University of Michigan and VA Medical Research Center, 2215 Fuller Road, Ann Arbor, Michigan 48105, United States

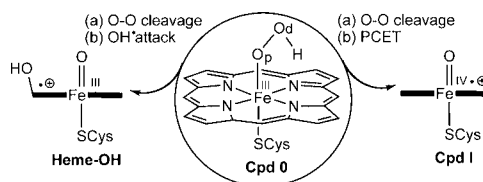
Supporting Information

ABSTRACT: The intriguing deactivation of the cytochrome P450 (CYP) 2B4 enzyme induced by mutation of a single residue, Phe429 to His, is explored by quantum mechanical/molecular mechanical calculations of the O–OH bond activation of the $(\text{Fe}^{3+}\text{OOH})^-$ intermediate. It is found that the F429H mutant of CYP 2B4 undergoes *homolytic instead of heterolytic* O–OH bond cleavage. Thus, the mutant acquires the following characteristics of a heme oxygenase enzyme: (a) donation by His429 of an additional NH---S H-bond to the cysteine ligand combined with the presence of the substrate retards the heterolytic cleavage and gives rise to homolytic O–OH cleavage, and (b) the Thr302/water cluster orients nascent OH^\bullet and ensures efficient meso hydroxylation.

Cytochrome P450s (CYPs) and heme oxygenase (HO) are O_2 -activating enzymes that convert O_2 to the ferric hydroperoxide species $[\text{Fe}^{3+}\text{OOH}^-]$, the so-called Compound 0 (Cpd 0) and then diverge in function. In the usual CYP function (Scheme 1), Cpd 0 abstracts a proton and splits off a water molecule to form the iron–oxo species Compound I (Cpd I), which oxidizes a wide range of organic compounds and performs biosynthesis.¹ In contrast, HO stops at Cpd 0 and uses it to activate the α -meso position of the porphyrin, which is subsequently degraded and frees iron, which is believed to be essential for iron homeostasis.² In both cases, water molecules play a major role; in CYPs, they shuttle protons to Cpd 0,^{3a} while in HO, a water cluster safeguards Cpd 0 against conversion to Cpd I and directs homolytic O–OH cleavage and meso hydroxylation by nascent OH^\bullet .^{3b} Considering the orthogonal functions of these enzymes, we report herein evidence that a single-site mutation converts the CYP 2B4 enzyme to a hybrid CYP/HO enzyme.

Our interest in this problem was triggered by a recent experimental study⁴ reporting that although cryoreduction of the oxyferrous complex in CYP 2B4 and its F429H mutant (MT) generated the same amounts of Cpd 0, the F429H MT exhibited only 4–5% product formation relative to the wild-type (WT) enzyme.^{4a} Thus, mutation of a single Phe residue near the cysteinate ligand (Phe429) to His leads to deactivation of the enzyme, apparently by disrupting conversion of Cpd 0 to Cpd

Scheme 1. Conversion of Cpd 0 to Cpd I versus the HO Option of Generating a Hydroxylated Heme



I. The position of the mutation near the cysteine ligand, along with the fact that Phe429 is a conserved P450 residue that plays a role in the electron-transfer pathway from the reductase to heme in CYP 2B4,^{4b} makes the outcome of the mutation intriguing and requires elucidation. We studied the impact of this mutation using hybrid quantum mechanics/molecular mechanics (QM/MM) calculations, which showed that the mutation leads to HO activity of the F429H MT enzyme as a result of a subtle interplay of electronic effects with changes caused by the substrate and the water structure in the active site.

The QM/MM study was carried out using our usual software combination^{5a–c} and followed the same protocols^{1b,5d} as in previous studies.^{3b,5e,f} Details are given in the Supporting Information (SI), and those more specific to the paper are given here briefly. Since Cpd 0 has been experimentally shown to exist in both the WT and MT enzymes, we started from the WT structure (PDB entry 1SUO),^{6a} replaced the inhibitor by the OOH group, added missing H atoms, took care of the protonation states of the acidic and basic residues,^{3b,5d,f} and followed with geometry optimization and molecular dynamics (MD) simulations. The F429H MT was initially generated by replacing Phe429 by His and then minimizing the protein. The resulting WT and MT enzymes were both found to generate Cpd I with minor quantitative differences in the barriers for heterolytic cleavage (Table S1, SI). We therefore extended the MD simulation to 60 ns and extracted from the MD trajectories the most highly sampled conformational basins,^{6b} called LW i and LM i , where L stands for long MD, W/M for the WT/MT enzyme, and i for the basin number. The WT enzyme prefers

Received: December 21, 2011

Published: February 22, 2012

conformations LW1 and LW3. Similarly, the MT enzyme prefers mostly LM3 and then LM1, while the unstable LM2 basin spontaneously decays to LM3 (Figure S1, SI). These most sampled conformations were used subsequently. Docking in the substrate (benzphetamine) and reoptimizing the enzymes led to expulsion of water from the pocket (Figures S2 and S3).^{4a,7} In LW1,3 and LM1–3, the water molecules mostly remained near the distal OH group of Cpd 0 near the Glu301 and Thr302 residues, which can shuttle protons to cause heterolytic cleavage.^{5e,8} Thus, as expected, the entrance of the substrate disfavors generation of H₂O₂ (“uncoupling”) via proximal-O protonation and prefers protonation of the distal OH group.⁹ The uncoupling barriers did not give a clue about the incapacitation of the MT enzyme. We therefore relegate the uncoupling processes to the SI (Figure S1, Tables S1 and S2) and focus herein on the O–OH cleavage using the conformations that retained water molecules in the pocket near Glu301 and Thr302. The QM/MM geometry optimization involved the QM system of the WT/MT enzyme and the residues and waters within 6 Å of the heme (~645 atoms; see the SI). As before,^{5e,8} the QM subsystem was computed with B3LYP^{10a} using a split-valence LACVP^{10b} basis set (B1) for geometry optimization and a triple- ζ valence-polarized (TZVP)^{10c} basis set (B2) for energy correction.

Figure 1 shows typical QM/MM-optimized snapshots for Cpd 0 of the WT and MT enzymes. It is evident that the two

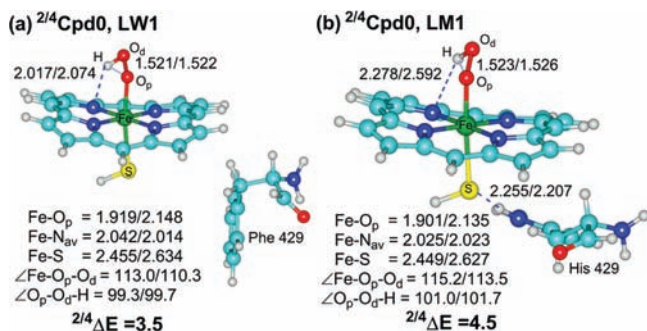


Figure 1. B3LYP-optimized geometries (Å and deg) and doublet/quartet energy gaps ${}^{2/4}\Delta E$ (kcal/mol) of Cpd 0 in conformations (a) LW1 and (b) LM1. The NH...S H-bond in (b) should be noted.

species are similar in their geometries, except for a trans effect in the MT enzyme (shorter Fe–O distance) caused by the additional H-bonding^{11a,b} between His429 and the S ligand (Figure 1b), thereby weakening its “push effect”.^{11c} In fact, the two Cpd 0 species have the same electronic structure and are similar in most respects, having a doublet-spin ground state and a quartet-spin excited state.^{5e,f} Thus, Cpd 0 gave no obvious clues about the mutation effect, so we next considered the features of the O–OH cleavage mechanisms.

As before,^{5e,f,8a} the O–OH cleavage process was scanned along the O–O distance with QM/MM optimization of all other parameters. The top of the scan was refined in a transition state (TS) search. Scheme 2 shows generic energy profiles of the two processes for the LW and LM conformations: one is Cpd I formation and the other is HO activity leading to meso hydroxylation of the heme.

Table 1 shows barriers and reaction energies for the two processes for the WT and MT enzyme conformations. The barriers are similar to ones computed previously for Cpd I formation.^{5e,f,8} However, while the two conformations of the

Scheme 2. Generic Energy Profiles Starting from Cpd 0 (Doublet Ground State) and Leading to (Right) Cpd I Formation and/or (Left) Meso Hydroxylation HO Activity

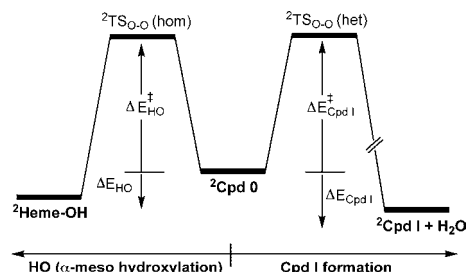


Table 1. Barriers and Reaction Energies (kcal/mol) for ${}^2\text{Cpd 0}$ to ${}^2\text{Cpd I}$ Conversion or HO Meso Hydroxylation

conformation	$\Delta E_{\text{Cpd I}}^\ddagger, \Delta E_{\text{Cpd I}}$	$\Delta E_{\text{HO}}^\ddagger, \Delta E_{\text{HO}}$
LW1	9.7, −27.8	not observed
LW3	16.0, −19.0	not observed
LM1	not observed	14.9, −6.1
LM3	not observed	17.4, −9.0
LM2	13.3, −10.7	not observed

WT enzyme lead to Cpd I formation, two of the three conformations of the MT enzyme lead to meso hydroxylation and the third (LM2) to Cpd I. Comparison of the barriers for Cpd I formation in the WT and MT enzymes shows that this process is not much affected by the mutation. *What is affected is the appearance of the HO mechanism in the MT enzyme in LM3 and LM1.* Since LM2 spontaneously decays to LM3, it follows that for the MT enzyme, the HO pathway competes favorably with Cpd I formation, while the WT enzyme favors Cpd I formation.

Importantly, the two processes compete along the same O–OH stretching coordinate. As before,^{5e,f,8a} we found that initially the O–OH bond breaks homolytically and then nascent OH[•] accepts an electron from the heme and a proton, which is shuttled from the acidic residue Glu301 through the water chain and Thr302, leading to Cpd I in a proton-coupled electron transfer (PCET) process.^{5e,f} When the PCET is interrupted by shortcutting the ET, nascent OH[•] can attack the meso position of the heme before it diffuses away.^{3b} Clearly, F429H mutation affects the PCET process of the MT enzyme, leading to a preference for the homolytic cleavage pathway.^{2a,3a}

Figure 2 shows the TS structures $\text{TS}_{\text{O-O}}(\text{het})$ for the heterolytic process leading to Cpd I in the WT conformations LW1 and LW3. Figure 3 shows the two TSs $\text{TS}_{\text{O-O}}(\text{hom})$ for the homolytic process leading to meso hydroxylation in the MT conformations LM1 and LM3 and $\text{TS}_{\text{O-O}}(\text{het})$ for LM2. An additional structure for LM3, I_H in Figure 3d, is an intermediate point along the O–O scan after $\text{TS}_{\text{O-O}}(\text{hom})$ and just before collapse to the meso hydroxylation product (a similar structure for LM1 is shown in Figure S4).

The heterolytic TS of the MT enzyme in Figure 3b is similar to those for the WT enzyme in Figure 2, except that the O–O distances in the WT enzyme (1.931 and 2.041 Å) are significantly shorter than the MT O–O distance (2.351 Å). This long O–O bond already shows diminished push effect due to the H-bonds to the thiolate. The long O–O distance also typifies the two $\text{TS}_{\text{O-O}}(\text{hom})$ structures in the MT enzyme (Figure 3a,c). Moreover, in the LM3 I_H structure in Figure 3d, nascent OH has a spin density of −0.99 and clearly is a radical.

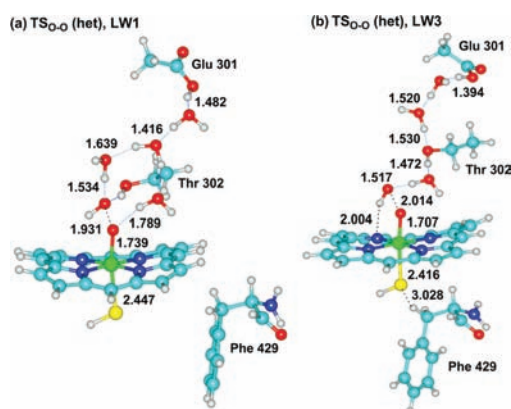


Figure 2. Key bond distances (Å) in the QM region in $\text{TS}_{\text{O-O}}(\text{het})$ for (a) LW1 and (b) LW3.

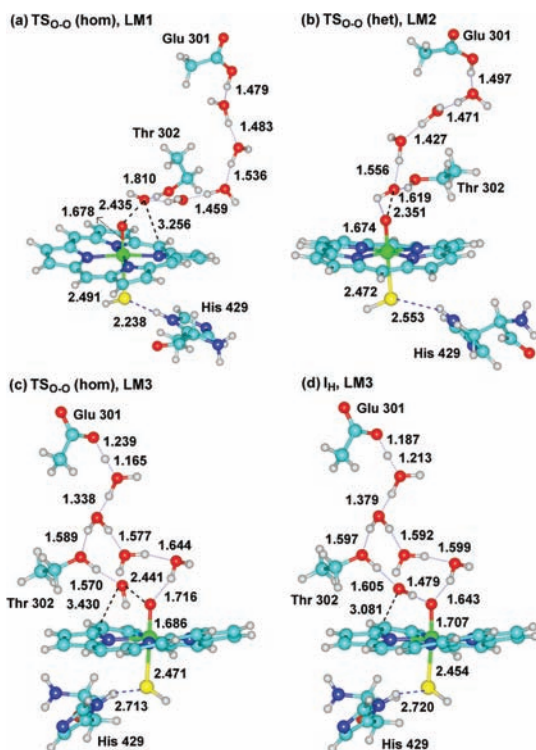


Figure 3. Key bond distances (Å) in (a) $\text{TS}_{\text{O-O}}(\text{hom})$ for LM1, (b) $\text{TS}_{\text{O-O}}(\text{het})$ for LM2, (c) $\text{TS}_{\text{O-O}}(\text{hom})$ for LM3, and (d) the homolytic intermediate structure I_{H} for LM3.

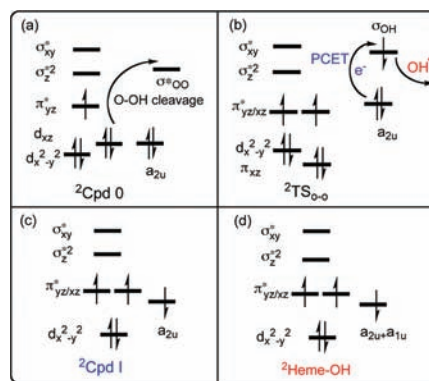
Thus, the proton- and electron-transfer events in the MT enzyme appear to lag behind the O–OH cleavage, so nascent OH^\bullet can either attack the meso position of the heme (Figure 3a,c) or be captured by the electron and proton to form Cpd I. On the other hand, as O–OH cleavage begins in the WT enzyme, the electron and proton capture nascent OH^\bullet and release it as water, giving it no chance to attack the heme.

The appearance of a competitive HO pathway in the mutant originates from the interplay of factors that adversely affect PCET: an electronic factor that delays ET to nascent OH^\bullet and a structural factor that holds the OH^\bullet moiety close to the meso position of the heme. The structural factor is apparent from Figure 3, which shows that Thr302 and the surrounding three water molecules hold nascent OH^\bullet quite close to the heme by an array of H-bonds (e.g., in Figure 3a, $\text{OH}\cdots\text{C}_{\text{meso}} = 3.256 \text{ \AA}$), precisely as observed in the original HO enzyme, where the

$(\text{H}_2\text{O})_6$ cluster orients OH^\bullet and forces it to stay close to the α -meso position of the porphyrin.^{2b,c,3b}

However, the structural factor by itself would be insufficient if there were no electronic effects that disrupt the PCET process by preventing the ET that converts the OH^\bullet to OH^- , which easily abstracts a proton. This effect is elucidated with aid of electron-shift diagrams: As the O–OH bond stretches (Scheme 3a), an electron initially in the iron d_{xz} orbital shifts to

Scheme 3. Electron-Shift Diagrams during (a) O–OH Cleavage of $^2\text{Cpd 0}$ and (b) PCET and OH Expulsion after $^2\text{TS}_{\text{O-O}}$, and Electron Configurations of the (c) $^2\text{Cpd I}$ and (d) $^2\text{Heme-OH}$ Products

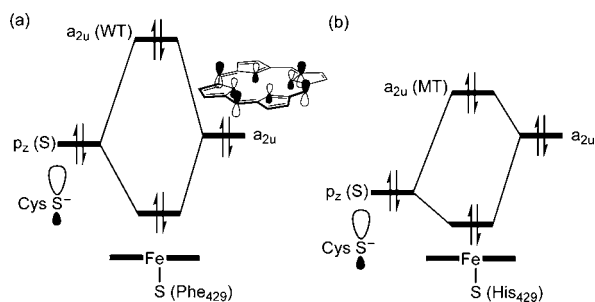


nascent OH^\bullet moiety, while the d_{xz} orbital becomes $\pi_{xz}^*(\text{FeO})$, thus forming a Compound II (Cpd II) ferryl species with a triplet configuration in the $\text{Fe}=\text{O}$ bond (Scheme 3b). This is what we found for all $\text{TS}_{\text{O-O}}(\text{het})$ and $\text{TS}_{\text{O-O}}(\text{hom})$ species: the electronic structure involves a triplet Cpd II antiferromagnetically coupled to an electron in a nascent OH^\bullet species. What matters is what transpires immediately afterward. At this juncture, when the a_{2u} orbital of porphyrin lies sufficiently high, an electron shifts to the σ_{OH} orbital of nascent OH^\bullet , which simultaneously accepts a proton from the nearby Glu/Thr proton channel to form Cpd I and a water molecule (Scheme 3c). In contrast, when the a_{2u} orbital is low-lying and the protein electric field is improperly oriented, the electron does not shift to σ_{OH} , and OH^\bullet (in red) instead attacks the porphyrin and generates a hydroxylated porphyrin (Scheme 3d).^{3b} What determines whether OH^\bullet attacks the porphyrin or diffuses away is the arrangement of the water cluster and the Thr302 residue, which in this 2B4 MT enzyme in the presence of the benzphetamine substrate appears to assume a directing effect, as does the protein² in the HO enzyme.

What factors stabilize the a_{2u} orbital in the MT enzyme and retard the ET? As mentioned above, the His429 residue maintains a $\text{NH}\cdots\text{S}$ H-bond to the S ligand (Figure 1b). This lowers the energy of the S $3p_\sigma$ orbital^{1b,12} and minimizes its mixing with the a_{2u} orbital (Scheme 4), which thus remains low in energy. Hence, significant O–OH cleavage is required for transfer of the requisite electron to nascent OH^\bullet . Additionally, entrance of the substrate, which expels and reorients water molecules, changes the direction of the intrinsic electric field that the MT protein exerts on the FeOOH moiety in such a way that the negative pole of the field in LM3 and LM1 is oriented in the direction of nascent OH^\bullet (Figures S5 and S6), thereby retarding the electron flow.¹³

Thus, the combination of the H-bond of His429 in F429H CYP 2B4 and the reorientation of the protein electric field in

Scheme 4. Qualitative MO Diagrams Showing the Mixing of the S Hybrid Orbital into the a_{2u} Orbital in (a) WT and (b) MT



LM1,3 disrupts the PCET process and enables homolytic O–OH cleavage to take over, producing the hybrid HO/CYP activity predicted here. This proposed impact of the H-bonding of His429 matches the recently reported blue-shift in absorption spectra of ferrous and ferric NO and ferrous CO complexes of the F429H mutant of CYP 2B4.¹⁴ The presence of Phe429 in the proximal side of CYP 2B4 (Figure 1a) near the cysteine ligand may have evolved to protect the sulfur from assuming too many H-bonds,^{11a,b} thereby regulating its “push effect”.^{11c} The fact that a proximal Phe is a conserved residue in CYPs may support the suggestion that Phe performs a regulatory function in modulating the redox potential of the heme^{14,15} so it can participate in the PCET process that leads to Cpd I formation, rather than allowing a homolytic O–OH cleavage. This fine-tuning of CYPs’ function by a single residue is a very intriguing feature of these enzymes. This delicate balance is highlighted by findings that the peroxide complexes of CYPs exhibit a mixture of homolytic and heterolytic bond cleavages^{3a,16} and even a propensity toward heme degradation.^{16b}

In conclusion, our QM/MM results show that MT enzyme F429H of CYP 2B4 develops characteristics of a HO enzyme: (a) its NH...S H-bond to the cysteine ligand and changes in the protein electric field induced by entrance of the substrate retard the heterolytic cleavage and result in a preference for homolytic O–OH cleavage; (b) its Thr302/water cluster and the bulky substrate structurally orient nascent OH• close to the porphyrin, enforcing meso hydroxylation. We have not explored other competitive processes (e.g., diffusion of OH• followed by H abstraction from the surrounding protein residues), nor did we consider H abstraction by the sulfur from His429 and generation of the inactive P420 form.¹⁴ Still, however, the meso hydroxylation is barrier-free, so the predicted HO activity should be observable.

■ ASSOCIATED CONTENT

Supporting Information

Tables S1–S6, Figures S1–S6, Cartesian coordinates, computational details, and complete refs 5a and 13a. This material is available free of charge via the Internet at <http://pubs.acs.org>.

■ AUTHOR INFORMATION

Corresponding Author

waskell@med.umich.edu; sason@yfaat.ch.huji.ac.il

Present Address

^{||}Department of Chemistry, Renmin University of China, Beijing, 100872, China.

Notes

The authors declare no competing financial interest.

■ ACKNOWLEDGMENTS

S.S. and L.W. were supported by NIH Grant R01-GM-094209 and L.W. by Veterans Administration Review Grant CC103. C.Z. thanks Hewlett-Packard for Computational facilities.

■ REFERENCES

- (1) (a) *Cytochrome P450: Structure, Mechanism and Biochemistry*, 3rd ed.; Ortiz de Montellano, P. R., Ed.; Kluwer: New York, 2004. (b) Shaik, S.; Cohen, S.; Wang, Y.; Chen, H.; Kumar, D.; Thiel, W. *Chem. Rev.* **2010**, *110*, 949.
- (2) (a) Colas, C.; Ortiz de Montellano, P. R. *Chem. Rev.* **2003**, *103*, 2305. (b) Unno, M.; Matsui, T.; Ikeda-Saito, M. *Nat. Prod. Rep.* **2007**, *24*, 553. (c) Matsui, T.; Unno, M.; Ikeda-Saito, M. *Acc. Chem. Res.* **2010**, *43*, 240.
- (3) (a) Denisov, I. G.; Makris, T. M.; Sligar, S. G.; Schlichting, I. *Chem. Rev.* **2005**, *105*, 2253. (b) Chen, H.; Moreau, Y.; Derat, E.; Shaik, S. *J. Am. Chem. Soc.* **2008**, *130*, 1953.
- (4) (a) Davydov, R.; Razeghifard, R.; Im, S.-C.; Waskell, L.; Hoffman, B. M. *Biochemistry* **2008**, *47*, 9661. (b) Hamdane, D.; Xia, C.; Im, S.-C.; Zhang, H.; Kim, J.-J. P.; Waskell, L. *J. Biol. Chem.* **2009**, *284*, 11374.
- (5) (a) Sherwood, P.; et al. *THEOCHEM* **2003**, 632, 1. (b) Brooks, B. R.; Burccoleri, R. E.; Olafson, B. D.; States, D. J.; Karplus, M. *J. Comput. Chem.* **1983**, *4*, 187. (c) Ahlrichs, R.; Bär, M.; Häser, M.; Horn, H.; Kölmel, C. *Chem. Phys. Lett.* **1989**, *162*, 165. (d) Senn, H. M.; Thiel, W. *Angew. Chem., Int. Ed.* **2009**, *48*, 1198. (e) Zheng, J.; Wang, D.; Thiel, W.; Shaik, S. *J. Am. Chem. Soc.* **2006**, *128*, 13204. (f) Chen, H.; Hirao, H.; Derat, E.; Schlichting, I.; Shaik, S. *J. Phys. Chem. B* **2008**, *112*, 9490.
- (6) (a) Scott, E. E.; White, M. A.; He, Y. A.; Johnson, E. F.; Stout, C. D.; Halpert, J. R. *J. Biol. Chem.* **2004**, *279*, 27294. (b) Zazza, C.; Amadei, A.; Palma, A.; Sanna, N.; Tatoli, S.; Aschi, M. *J. Phys. Chem. B* **2008**, *112*, 3184.
- (7) (a) Mak, P. J.; Im, S.-C.; Zhang, H.; Waskell, L.; Kincaid, J. R. *Biochemistry* **2008**, *47*, 3950. (b) Mak, P. J.; Zhang, H.; Hollenberg, P. F.; Kincaid, J. R. *J. Am. Chem. Soc.* **2010**, *132*, 1494.
- (8) (a) Altarsha, M.; Benighaus, T.; Kumar, D.; Thiel, W. *J. Am. Chem. Soc.* **2009**, *131*, 4755. (b) Sen, K.; Hackett, J. C. *J. Phys. Chem. B* **2009**, *113*, 8170.
- (9) (a) Makris, T. M.; von Koenig, K.; Schlichting, I.; Sligar, S. G. *Biochemistry* **2007**, *46*, 14129. (b) Vatsis, K. P.; Peng, H.-W.; Coon, M. J. *J. Inorg. Biochem.* **2002**, *91*, 542. (c) Raag, R.; Poulos, T. *Biochemistry* **1989**, *28*, 7586.
- (10) (a) Becke, A. D. *J. Chem. Phys.* **1993**, *98*, 5648. (b) Hay, P. J.; Wadt, W. R. *J. Chem. Phys.* **1985**, *82*, 299. (c) Schäfer, A.; Huber, C.; Ahlrichs, R. *J. Chem. Phys.* **1994**, *100*, 5829.
- (11) (a) Poulos, T. L. *J. Biol. Inorg. Chem.* **1996**, *1*, 356. (b) Yoshioka, S.; Takahashi, S.; Ishimori, K.; Morishima, I. *J. Inorg. Biochem.* **2000**, *81*, 141. (c) Dawson, J. H. *Science* **1988**, *240*, 433.
- (12) (a) Oglario, F.; de Visser, S. P.; Shaik, S. *J. Inorg. Biochem.* **2002**, *91*, 554. (b) Shaik, S.; Hirao, H.; Kumar, D. *Nat. Prod. Rep.* **2007**, *24*, 533.
- (13) (a) Cho, K.-B.; et al. *J. Phys. Chem. A* **2008**, *112*, 13128. (b) See the equation in Table S1 of: Lai, W. Z.; Chen, H.; Cho, K.-B.; Shaik, S. *J. Phys. Chem. Lett.* **2010**, *1*, 2082.
- (14) Perera, R.; Sono, M.; Kinloch, R.; Zhang, H.; Tarasev, M.; Im, S.-C.; Waskell, L.; Dawson, J. H. *Biochim. Biophys. Acta* **2011**, *1814*, 69.
- (15) Ost, T. W. B.; Miles, C. S.; Munro, A. W.; Murdoch, J.; Reid, G. A.; Chapman, S. K. *Biochemistry* **2001**, *40*, 13421.
- (16) For example, see: (a) Reference 3a and discussions therein. (b) White, R. E.; Sligar, S. G.; Coon, M. J. *J. Biol. Chem.* **1980**, *255*, 11108. (c) Shimizu, T.; Murakami, Y.; Hatano, M. *J. Biol. Chem.* **1994**, *269*, 13296.